

Evaluation of Structure Development of Xanthan and Carob Bean Gum Mixture Using Non-Isothermal Kinetic Model

Won Byong Yoon and Sundaram Gunasekaran^{1*}

Firmerich Asia Private Limited, 10 Tuas West Road, Singapore 638377, Singapore

¹Food and Bioprocess Engineering Laboratory, Department of Biological Systems Engineering, University of Wisconsin-Madison, Madison, WI 53706, USA

Abstract Gelation mechanism of xanthan-carob mixture (X/C) was investigated based on thermorheological behavior. Three X/C ratios (1:3, 1:1, and 3:1) were studied. Small amplitude oscillatory shear tests were performed to measure linear viscoelastic behavior during gelation. Temperature sweep (-1°C/min) experiments were conducted. Using a non-isothermal kinetic model, activation energy (E_a) during gelation was calculated. At 1% total concentration, the E_a for xanthan fraction (ϕ_x)=0.25, 0.5, and 0.75 were 178, 159, and 123 kJ/mol, respectively. However, a discontinuity was observed in the activation energy plots. Based on this, two gelation mechanisms were presumed-association of xanthan and carob molecules and aggregation of polymer strands. The association process is the primary mechanism to form 3-D networks in the initial stage of gelation and the aggregation of polymer strands played a major role in the later stage.

Keywords: xanthan gum, carob bean gum, rheology, gelation, kinetics

Introduction

Polysaccharides are one of the most abundant biopolymers used in food industries. They are capable of forming an infinite 3-dimensional network entrapping water and other constituents. Foods incorporate polysaccharides either as major components or as a part of a multicomponent system offer wide range of functionalities due to both structural and mechanical properties. In addition, polysaccharide systems can have synergistic interactions by mixing with two or more components together (1). Studies of mixed polysaccharide systems are more realistic models for foods and becoming more important due to the recent interest in developing self-textured foods as an alternative to the use of additives (2).

Theories to explain molecular interactions and structure development during thermally induced gelation have been developed and tested for many single biopolymer gels. Since mixing biopolymers is a recent trend to modify physical properties of the resultant gels, study of mixed biopolymer gel systems is more realistic models for foods (3). Such theories to describe rheological behavior of mixed system are needed. However, multiplicity of structures in mixed gel systems makes it difficult to characterize their structure and properties.

Xanthan gum is produced by microbial fermentation process. Xanthan (X) and carob (C) gums enhance the solution viscosity in dispersed state and are commonly used as stabilizers/thickeners in food formulations (4). Though they do not form stable gels independently, they synergistically form a stable gel network when used together. The weak interactions between xanthan and carob (X/C) mixture are sensibly influenced by thermal

treatment. Such unique gelling behavior is used in food industries to control the quality of final products.

Many studies have proposed to describe the synergistic interactions between X and C (4, 5). In general, the synergistic gelation results from the combination of xanthan helix and unsubstituted region of the galactomannan backbone. However, due to the complicated structure of xanthan, these interactions, especially the mixing ratio dependence during gelation, are not well understood (4, 5).

Structure development rate (SDR) during gelation can be measured under isothermal and non-isothermal conditions by measuring rheological properties. For example, under non-isothermal conditions rheological data from temperature sweep experiments can be used to estimate SDR as the rate of change of storage modulus, G' (i.e., dG'/dt). The SDR of protein system has been investigated using the non-isothermal kinetic models (6).

Temperature is the only thermodynamic parameter involved in most gelation processes at a given biopolymer concentration. Therefore, the gelation mechanism and structure development can be analyzed by interpreting thermal effects on rheological property changes. Depending on the molecular configuration of the polymer network, temperature can have different effects on viscoelastic behavior of the gel.

The objectives of this study were to: 1) characterize thermal effects on the gelation process, and 2) propose possible gelation mechanisms based on thermal and rheological properties.

Materials and Methods

Materials Laboratory grade X and C were purchased (Sigma Chemical Co., St. Louis, MO, USA). Three xanthan-to-carob (X/C) ratios, 1:3, 1:1, and 3:1, were used. The total polymer concentration of 0.5% (0.5 g in 100 mL of 0.1 M NaCl solution) was maintained for all

*Corresponding author: Tel: +1-608-262-1019; Fax: +1-608-262-1228

E-mail: guna@wisc.edu

Received April 30, 2007; accepted July 8, 2007

mixtures. De-ionized water was used for gel preparation. The X and C powders were solubilized separately in water at 95°C by stirring for 30 min. The solutions were then blended at 85°C and mixed for 30 min and used in experiments.

Rheological measurement Small amplitude oscillatory shear (SAOS) tests were performed using the cone-and-plate (4/40) geometry in a dynamic rheometer (CVO, Bohlin Instruments Ltd., Cranbery, NJ, USA). To prevent moisture loss during experiments, mineral oil was applied around the sample edge.

Temperature sweep tests (at 0.1 Hz) were conducted to obtain the viscoelastic properties during gelation by *in situ* cooling of the gel mixture from 75 to 25°C at a rate of -1°C/min. The storage modulus (G') was recorded. All experiments were performed in the linear viscoelastic region by setting the target strain=0.02, determined experimentally by strain sweep test of the 1:1 mixture at 75°C, the highest temperature during experiment (Fig. 1). The linear range was operationally defined as the strain value at 95% of the G' at equilibrium during strain sweep test, as shown in Fig. 1. (7-9)

Non-isothermal kinetic model The general expression for non-isothermal kinetics is as follows:

$$\int_{C_0}^C \frac{dC}{C^n} = k_0 \int_0^t \exp\left(-\frac{Ea}{RT(t)}\right) dt \quad (1)$$

where, C =concentration, C_0 =initial concentration, t =time, k_0 =frequency factor, Ea =the activation energy (J/mole), T =absolute temperature (K), n =kinetic order and, R =universal gas constant (8.314 J/mol·K). The finite value of concentration or physical properties at a certain temperature during heating or cooling process can be expressed in a single kinetic model, and the kinetic parameter at each temperature can be compared by combining with the Arrhenius theory. The infinitesimal

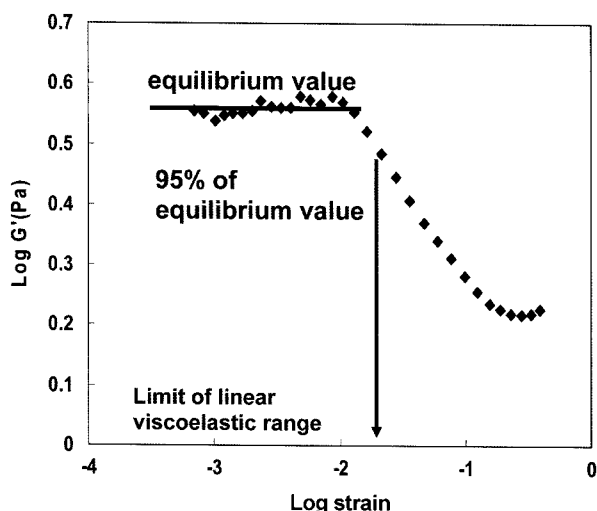


Fig. 1. Profiles of strain dependence of storage modulus of X/C (1:1) mixture at 75°C. The limit of linear viscoelastic range was operationally determined at 95% of equilibrium value.

value of temperature increment during the continuous heating or cooling process can be numerically integrated from initial to final conditions. Such numerical integration of a kinetic model represents the accumulation of changes of concentration or physical properties during continuous heating or cooling process (10-12).

The kinetic parameters have been obtained by following algorithm applied in Yoon *et al.* (6). For the decomposition reaction, the rate of reaction is given by:

$$-\frac{dC}{dt} = kC^n \quad (2)$$

The temperature dependence of reaction rate constant k is given by the Arrhenius relation:

$$k = k_0 \exp\left(-\frac{Ea}{RT}\right) \quad (3)$$

Absolute temperature (T) can be written in terms of time (t) at a constant linear heating rate:

$$T = T_0 + At \quad (4)$$

where T_0 =initial temperature (K) and A =heating rate (K/sec). By differentiating Eq. 4, the heating rate and infinitesimal time increase (dt) are expressed as:

$$A = \frac{dT}{dt} \quad (5a)$$

$$dt = \frac{dT}{A} \quad (5b)$$

Combining Eq. 5a and 5b with Eq. 2 and 3 yields:

$$-\frac{A}{C^n} \frac{dC}{dT} = k_0 \exp\left(-\frac{Ea}{RT}\right) \quad (6a)$$

$$\ln\left(-\frac{A}{C^n} \frac{dC}{dT}\right) = \ln k_0 - \frac{Ea}{RT} \quad (6b)$$

The derivative of concentration with respect of temperature in the Eq. 6b can be replaced with the time derivative (Eq. 5a), if the heating rate is a linear function of time. Then, Eq. 6b can be rewritten as:

$$\ln\left(-\frac{1}{C^n} \frac{dC}{dt}\right) = \ln k_0 - \frac{Ea}{RT} \quad (7)$$

The kinetic parameters, k_0 and Ea are determined from an Arrhenius-type plot of Eq. 7.

Results and Discussion

Gelation of X/C mixture The X, C, and X/C mixture showed a typical heat reduced gelation (Fig. 2). At high temperature, G' values of all combination are much lower than that of low temperature. G' of pure X and C solutions did not show any appreciable increase during the temperature sweep from 75 to 25°C. However, G' of the X/C mixtures increased dramatically at slightly lower than 55°C. The dramatic increase in G' of the X/C mixture indicates that there is a phase transition from sol to gel during cooling. This may be due to the interaction between X and galactomannan groups of carob at low temperature. Because of the conformational transition of X molecules

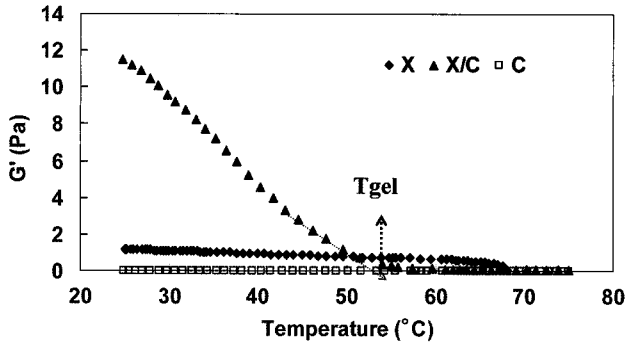


Fig. 2. Storage modulus (G') of xanthan (X) and carob (C), and 1:1 xanthan-carob (X/C) mixture during cooling from 75 to 25°C at 1 Hz. (Tgel: the gelation temperature)

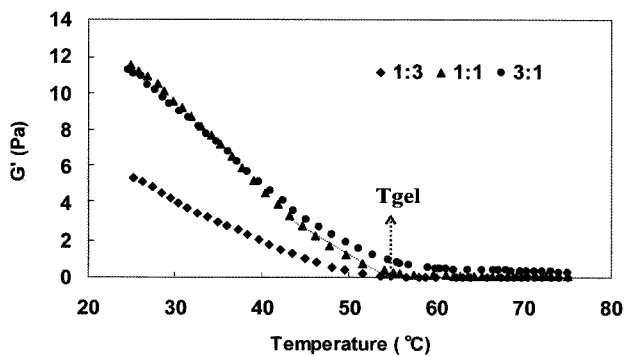


Fig. 3. Changes in storage modulus (G') of different X/C mixtures (1:3, 1:1, 3:1) during temperature sweep from 75 to 25°C. (Tgel: the gelation temperature)

from random coil to double helix at 55°C (2, 4), the sol to gel transition begins near 55°C.

Effect of mixing ratio The dependence of rheological properties on X/C ratio during cooling process, is shown in Fig. 3. At all X/C ratios studied, the typical gelation behavior described earlier was observed-increasing moduli with a phase transition at slightly lower than the configurationally transition temperature of xanthan 55°C. The sensitivity of mixing ratio of X/C was explained based on the junction zone model. The probability of interacting xanthan helix with unsubstituted backbone is dependent on the X/C ratio at constant polymer concentration (4, 5, 13). The xanthan fraction (ϕ_x) had a strong effect on the synergistic interaction (as measured by increasing G') as the ϕ_x changed from 0.25 to 0.5 (i.e., 1:3 to 1:1 X/C ratio). When $\phi_x > 0.5$, the ϕ_x fraction does not seem to positively contribute to the gel strength beyond what was observed at $\phi_x = 0.5$. Thus, 1:1 mixing of xanthan and carob can be considered the optimal ratio to facilitate the most synergistic interactions (4, 5, 13).

The gelation temperature of different ratio of X/C was slightly dependent on the X/C ratio. Higher ϕ_x shows higher gelation temperature. It may be because the higher probability of finding a suitable molecular pair to form X/C association in higher xanthan portion after the configurational changes of xanthan molecules from random coils to ordered helices around 55°C.

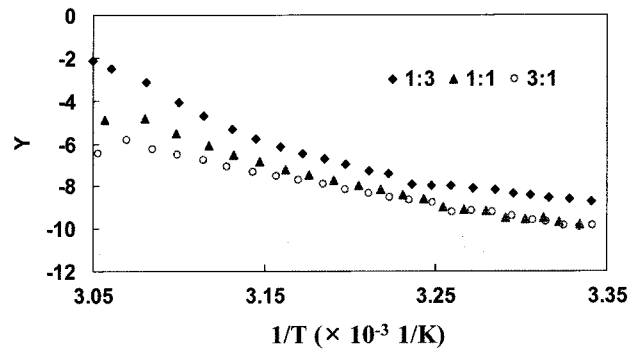


Fig. 4. Arrhenius-type plot relating rate of change in storage modulus and inverse of absolute temperature ($1/T$) during cooling of different X/C mixtures 1:3, 1:1, and 3:1. ($Y = \ln [(1/G^2)(dG'/dt)]$, G' =storage modulus)

Table 1. Activation energy estimated for xanthan-carob (X/C) mixed gel from the non-isothermal kinetic model

X/C ratio	Discontinuity temperature ¹⁾ (°C)		Activation energy (kJ/mol)		
	T ₁	T ₂	55-25	55-T ₁	T ₂ -25
1:3	43.4	33.7	178.81 (R ² =0.96)	329.32 (R ² =0.99)	93.43 (R ² =0.98)
1:1	38.9	34.0	159.23 (R ² =0.97)	197.84 (R ² =0.99)	83.05 (R ² =0.97)
3:1	34.0	34.0	118.21 (R ² =0.98)	120.13 (R ² =0.99)	83.55 (R ² =0.97)

¹⁾T₁, temperature at the end of the first linear segment; T₂, temperature at the beginning of the second linear segment.

Non-isothermal kinetic model When the macroscopic behavior (storage modulus) is solely a function of the statistical quantity of the microscopic contribution (i.e., chemical aggregation), the gelation mechanism can be expressed by a non-isothermal kinetic model based on the combination of the Arrhenius equation and time-temperature relationship shown in Rhim *et al.* (10). The aggregation of macromolecules was assumed to be described by a bimolecular association equilibrium, i.e., $n=2$ (6, 9).

The activation energy (E_a) for the gelation process was calculated from the non-isothermal kinetic model (Eq. 7). The semi-logarithmic plot of the left hand side of Eq. 1 vs. inverse of absolute temperature ($1/T$) is shown in Fig. 4. The slope of this linear plot is E_a/R . However, as can be observed, the plots are not linear. The best-fit lines were used to obtain slopes and calculate E_a (Table 1).

In addition, two linear segments were considered: 55°C to T₁ and T₂ to 25°C, where T₁ and T₂ are end of the first and beginning of the second linear segment, respectively (Fig. 5). The gap between T₁ and T₂ represents a discontinuity in the activation energy. The discontinuity temperatures T₁ and T₂ were determined based on best-fit linear regression models such that the R² values were maximized for both line segments for each X/C mixture. This discontinuity was dependent on ϕ_x . The E_a values for each linear segment were calculated and summarized in

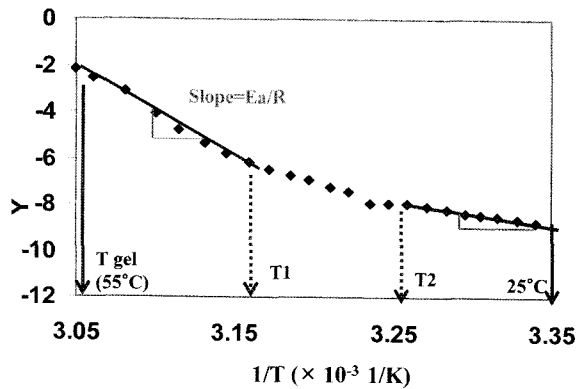


Fig. 5. The illustration of the discontinuity of activation energy for the 1:3 X/C mixture. ($Y = \ln [(1/G^2)(dG^2/dt)]$, G^2 = storage modulus)

Table 1 along with the T_1 and T_2 . When $\phi_X=0.25$ the discontinuity was observed between 43.4 (T_1) and 33.7°C (T_2), and E_a at the first region (from gelation temperature, about 55°C to T_1) and the second region (from T_2 to 25°C) was 329 and 93 kJ/mol, respectively.

Based on the discontinuity in E_a , two processes may be presumed, each with different temperature dependence. The initial intermolecular local contact is essentially by hydrogen bonding and involves short chain segments as well as configurational changes from random coil state to the ordered double helix region of xanthan strands (14). This process is considered the primary gelation mechanism above T_1 . The second process (T_2 to 25°C) is attributed to lateral aggregation processes of chain strands and growth of junction zones (15, 16). This is essentially governed by the hydrophobic interaction, favored by increasing temperature. This is considered the primary mechanism in the T_2 to 25°C range.

We may speculate on the physical nature of these cross-links by assuming that they are mainly due to hydrogen bonding between chains. The heat of hydrogen bonding formation is about 5 kcal/mol (20.92 kJ/mole) (9). Then, according to the values listed in Table 1, each cross-link may consist of about 5 to 10 hydrogen bonds, depending on the relative stability.

In terms of E_a values calculated for the entire range (55 to 25°C) and for two discontinuous temperature ranges, it is clear that, as ϕ_X increased, E_a values decreased (Table 1). Since E_a value can be considered as the energy barrier for the gelation process, increasing ϕ_X facilitates a more favorable gelation process. In the 55°C to T_1 region, the decrease in E_a was more substantial when the ϕ_X changed from 0.25 to 0.5, rather than from 0.5 to 0.75 indicating a strong synergism until $\phi_X=0.5$. In fact, increasing the ϕ_X beyond 0.5 level does not result in an increase in the E_a value in the T_2 to 25°C ranges.

In addition, ϕ_X also seems to affect the discontinuity gap (T_1-T_2). In general, as ϕ_X increased the gap steadily decreased. In the case of $\phi_X=0.75$, the discontinuity was almost nonexistent. The dependence of discontinuity gap

on ϕ_X implies that two gelation mechanisms may overlap at high ϕ_X . It might imply that the xanthan portion in the mixture dominated the initial intermolecular contact during reaction. This study will be useful for controlling textural properties of gel products in many food industries (17-19).

References

- Ridout MJ, Brownsey GJ. Rheological characterization of biopolymer mixed gels. pp. 577-587. In: Gums and Stabilizers for the Food Industry 3. Phillips GO, Wedlock DJ, Williams PA (eds). Elsevier Applied Science Publishers, New York, NY, USA (1986)
- Morris VJ. Weak and strong polysaccharide gels. pp.310-321. In: Food Polymers, Gels, and Colloids. Dickinson E (ed). The Royal Society of Chemistry, Cambridge, UK (1991)
- Sperling LH. Introduction to Physical Polymer Science. John Wiley & Sons, Inc., New York, NY, USA. pp.159-380 (1992)
- Urlacher B, Noble O. Xanthan gum. pp. 284-311. In: Thickening and Gelling Agents for Food. 2nd ed. Imeson A (ed). Blackie Academic and Professional, New York, NY, USA (1992)
- Morris ER. Mixed polymer gels. pp. 327-344. In: Food Gels. Harris P (ed). Elsevier Applied Science, New York, NY, USA (1990)
- Yoon WB, Gunasekaran S, Park JW. Characterization of thermo-rheological behavior of Alaska pollock and pacific whiting surimi. J. Food Sci. 69: E338-343 (2004)
- Yoon WB. Rheological characterization of biopolymer mixtures. PhD thesis, University of Wisconsin-Madison, Madison, WI, USA (2001)
- Shih WH, Shih WY, Kim SI, Liu J, Aksay IA. Scaling behavior of the elastic properties of colloidal gels. Phys. Rev. A 42: 4772-4779 (1990)
- Ould Eleya MM, Ko S, Gunasekaran S. Scaling and fractal analysis of viscoelastic properties of heat-induced protein gel. Food Hydrocolloid 18: 315-423 (2004)
- Rhim JW, Nunes RV, Jones VA, Swartzel KR. Determination of kinetic parameters using linearly increasing temperature. J. Food Sci. 54: 446-450 (1993)
- Hill CG Jr. An Introduction to Chemical Engineering Kinetics and Reactor Design. Wiley, New York, NY, USA. pp. 5-75, 349-388 (1977)
- Ahmed J, Ramaswamy HS, Ayad A, Intez A. Thermal and dynamic rheology of insoluble starch from basmati rice. Food Hydrocolloid 22: 278-287 (2008)
- Mao C-F, Rwei S-P. Cascade analysis of mixed gels of xanthan and locust bean gum. Polymer 47: 7980-7987 (2006)
- Eldridge JE, Ferry JD. Studies of the cross-linking process in gelatin gels. III. Dependence of melting point on concentration and molecular weight. J. Phys. Chem. 58: 992-995 (1954)
- Morris VJ. Gelation of polysaccharides. pp.141-226. In: Functional Properties of Food Macromolecules. 2nd ed. Hill SE, Ledward DA, Mitchell JR (eds). An Aspen Publication, Gaithersburg, MD, USA (1998)
- Lopes da Silva JA, Rao MA, Fu J-T. Rheology of structure development and loss during gelatin and melting. pp.111-157. In: Phase/State Transitions in Food. Rao MA, Hartel RW (eds). Marcel and Dekker, Inc., New York, NY, USA (1998)
- Lee SY, Kim JY, Lee SJ, Lim ST. Textural improvement of sweet potato starch noodle prepared without freezing using gums and other starches. Food Sci. Biotechnol. 15: 986-989 (2006)
- Hong GP, Park SH, Kim JY, Lee SK, Min SG. Effects of time-dependent high pressure treatment on physico-chemical properties of pork. Food Sci. Biotechnol. 14: 808-812 (2005)
- Choi YM, Ryu YC, Lee SH, Kim BC. Relationships between myosin light chain isoforms, muscle fiber characteristics, and meat quality traits in porcine longissimus muscle. Food Sci. Biotechnol. 14: 639-644 (2005)